Narrative Review Article

Physical Perturbations of the Circular Restricted Three-Body Problem: Effects on Equilibria and Periodic Orbits

Hristo A. Hristov

Sofia High School of Mathematics, Sofia Center Ul. Iskar 61, Sofia, 1000, Bulgaria

ABSTRACT

The circular restricted three-body problem (CR3BP) is a standard astrophysical model, yet real systems deviate from its ideal assumptions. This article is a narrative review and synthesis of previous literature on how three perturbation classes: radiation pressure, oblateness, and drag, modify equilibria and periodic-orbit families in CR3BP dynamics. For conservative perturbations, equilibrium locations and stability become multi-parameter problems: radiation can admit nonclassical out-of-plane equilibria and, in special luminous-binary regimes, stable L1; two-oblateness models replace a single stability threshold with numerically mapped stability boundaries. Correspondingly, major periodic-orbit families generally persist but deform, so the main outputs are continuation branches and stability maps. In contrast, dissipative drag produces displaced equilibria and prevents persistence of conservative periodic families; reported behavior is commonly transient decay. These results translate directly into modeling guidance for libration-point mission design and for predicting co-orbital capture and decay of small bodies in drag-dominated environments.

Keywords: restricted three-body problem; Lagrange point; radiation pressure; oblateness; drag force; periodic orbits

INTRODUCTION

Gravitational motion in three-body systems is a foundational problem in celestial mechanics and remains central to both theoretical dynamics and applications. The general three-body problem historically motivated deep developments in dynamical systems (1) but is non-integrable in closed form (2, 3), therefore, many practical questions can be addressed through simplified models that preserve the key geometric structures controlling transport and stability. An important one is the CR3BP, in which two massive primaries move on circular orbits about their barycenter and a third body of negligible mass evolves under their gravity (4–6). In a uniformly rotating frame, the primaries are fixed on the x-axis, and the motion is organized by an effective potential with Coriolis terms.

A defining feature of the CR3BP is the existence of five equilibrium (libration) points, L1–L5, where the net acceleration vanishes in the rotating frame (7). Figure 1 provides the geometric setup used throughout this review: the mass parameter $\mu = m_2 / (m_1 + m_2)$, the locations of the primaries, and the five equilibrium points that organize nearby motion. Linearization about these equilibria determines local stability properties and the nearby families of oscillatory motion (8). In the unperturbed CR3BP, the Jacobi integral further

Corresponding author: Hristo A. Hristov, E-mail: iceto113@gmail.com.

Accepted January 26, 2026
https://doi.org/10.70251/HYJR2348.41457466

constrains admissible regions of motion via zero-velocity curves and surfaces (9).

These invariant structures underpin modern trajectory design near equilibrium points (families of Lyapunov and Halo orbits used in operational mission geometries) and they also help explain natural co-orbital populations. Figure 2 illustrates this connection by showing a representative Lyapunov-orbit family about L1: such families emerge from the linearized dynamics near the collinear equilibria and persist into nonlinear regimes.

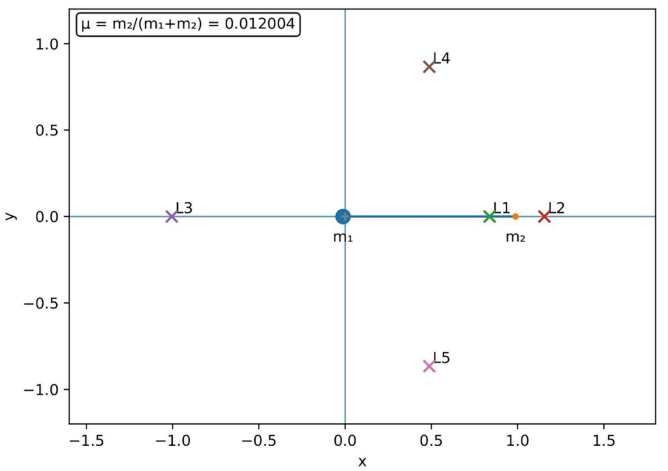

Figure 1. *A simple restricted three-body system, defined by the parameter μ = m₂ / (m₁ + m₂), with the locations of the primaries and the Lagrange points. Original figure created by the author.*

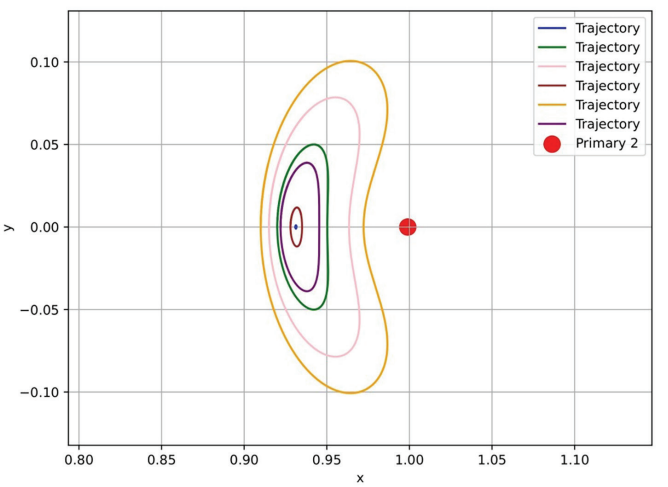

Figure 2. *Representative Lyapunov orbit family around L1 computed using a shooting method; trajectories plotted in Python Matplotlib. Original figure created by the author.*

In applied settings, libration-point dynamics has been exploited since early work on libration-point satellites (10), while in natural systems the triangular equilibria motivate explanations of Trojan-like populations (11).

At the same time, the standard CR3BP assumptions are rarely exact. Real primaries can deviate from point-mass gravity through oblateness (12) and related non-spherical terms; luminous bodies exert radiation forces that modify effective attraction (13–15); and in some astrophysical contexts the primaries' masses may vary in time (16). Dissipative environments introduce an additional qualitative change: drag forces break energy-like invariants and can convert classical equilibria into drag-displaced fixed points whose location and stability depend on the specific force law (17, 18). Even when perturbations are small, the literature shows that they can shift equilibrium locations, reshape stability boundaries, deform periodic-orbit families, and alter the transport pathways implied by the classical CR3BP's invariant structures (13, 19).

This article reviews how three representative perturbation classes modify equilibria and periodic orbits within this framework, with emphasis on what changes qualitatively, what can be obtained analytically, and what typically requires numerical computation. Radiation-pressure models provide a conservative multi-parameter classification of equilibrium existence and linear stability (13), while oblateness modifies Trojan-point stability thresholds and can turn the classical single critical mass ratio into a multi-parameter boundary (19). Beyond equilibrium structure, combined-perturbation studies highlight how periodic and resonant families deform under radiation or oblateness and how analytical expansions and numerical mapping complement each other in practice (20, 21). The goal of the review is to synthesize these threads into a comparative picture that supports both interpretation and use: what each perturbation does to the CR3BP's organizing structures, which methods are reliable across parameter regimes, and where the literature has left gaps for future research.

PERTURBATION EFFECTS ON EQUILIBRIA

Radiation pressure

Radiation pressure is commonly incorporated in the CR3BP via the photogravitational model, where radiation from each primary is treated as a conservative rescaling of its inverse-square attraction. The resulting "mass-reduction factors" are often denoted by q_1 and q_2 (one for each primary), with $q_i = 1$ recovering the classical

CR3BP and $q_i < 1$ representing reduced effective gravity due to outward radiation. In Simmons *et al*., these same parameters are written as α, β; throughout this review we use $q_1 \equiv \alpha$, $q_2 \equiv \beta$. When geometric interpretations are helpful, we also use the "cube-root" parameters $\delta_i = q_i^{1/3}$, which enter naturally in equilibrium-distance relations.

In this conservative formulation, the primaries' circular motion is unchanged and radiation enters only through the effective potential. Equilibria therefore remain stationary points of an effective potential, but their locations and linear stability become functions of the three-parameter set (μ, q_1, q_2) rather than of μ alone. Relative to the classical geometry in Figure 1, radiation shifts the collinear points along the x-axis and displaces the triangular points in both x and y.

Early development established the equilibrium-displacement picture without a modern global classification. Radzievskii first formulated the restricted problem with light pressure and analyzed how radiation reshapes Roche surfaces and displaces collinear equilibria (22). Radzievskii later extended the equilibrium discussion but still did not provide a systematic linear-stability classification (23). Chernikov subsequently treated linear stability of L1–L5 within the photogravitational model, and Perezhogin later analyzed out-of-plane equilibria (often denoted L6 and L7 in later notation) in the Sun–planet limit and found them unstable there (15, 24). Schuerman then considered the case where both primaries radiate, but later authors argued that parts of that treatment were incomplete, particularly in high-luminosity regimes and in the handling of collinear and out-of-plane equilibria (14).

The most complete classification is the global existence-and-stability work of Simmons *et al*., which treats arbitrary μ and arbitrary radiation parameters from both primaries (13). Their results can be summarized by grouping outcomes into geometry, stability, and nonclassical equilibria.

For L4 and L5, it can be shown that equilibrium distances satisfy simple relations that admit a clear geometric interpretation (circle–circle intersections with radii set by the radiation parameters). A key qualitative feature is a degenerate boundary: when the relevant equality condition holds, L4 and L5 collapse onto the x-axis and become degenerate with the inner collinear equilibrium L1, which is easiest to visualize using the classical layout in Figure 1 (13).

For fixed μ, the linear-stability region of L4 and L5 becomes a restricted subset of the (q_1, q_2) plane and can be represented geometrically. For collinear equilibria, the classical "all unstable" picture changes only partially: L2 and L3 remain unstable for all mass ratios and radiation parameters, but L1 can become linearly stable inside a bounded region that requires both primaries to exert radiation pressure (13).

Additionally, up to four out-of-plane equilibria (L6-L9) can exist when the radiation parameters satisfy constraints, such as radiation-dominated regimes. A mapping of existence regions in radiation-parameter space (Figure 3) has been done, and it can be shown that stability is highly restricted: L8, L9 are always unstable when present, while L6, L7 admit stability only in a limited parameter window (13).

Finally, Simmons *et al*. (13) comment on physical relevance: the most distinctive new behaviors (particularly stable L1 and the stable window for L6 and L7) are expected only when both primaries are luminous and of comparable mass, as in certain binary systems; they suggest, for example, that L1 stability may be relevant to mass transfer in binaries.

Oblateness

The standard way to model oblateness in celestial mechanics comes from potential theory. The gravitational potential of an axisymmetric body reduces to a zonal-

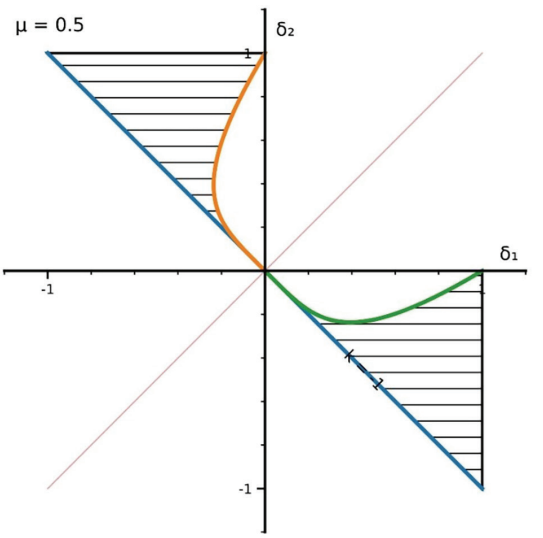

Figure 3. *Out-of-orbital-plane equilibrium points existence for $\mu = 0.5$ (13). Inside the shaded region, there is a single equilibrium point above the orbital plane and a corresponding one below it; outside that region, no such solutions occur. Along the line, the equilibrium lies on $y = 0$, $z = 0$. Replotted by the author based on parameter map described in (13).*

harmonic series expressed using Legendre polynomials (25). Truncating the expansion at the leading non-spherical correction yields the familiar quadrupole term, written with the coefficient J_2, which captures rotational flattening. The potential then is defined with an infinite sum where J_n is the n-th coefficient, R is the equatorial radius of the body, M is its mass, and θ is the colatitude.

In artificial-satellite dynamics, this leading J_2 correction is the standard first-order departure from point-mass gravity, with classical analytical treatments by Brouwer (26) and Kozai (27).

This same model was later imported into the restricted three-body setting by adding a J_2-type correction to the effective potential of one (or both) primaries (in the rotating reference frame):

$$\Omega(x,y) = \frac{1}{2}(x^2 + y^2) + \frac{1-\mu}{r_1} + \frac{\mu}{r_2} + \frac{(1-\mu)A_1}{2\,r_1^3} + \mu\frac{A_2}{2\,r_2^3}$$

$$A_i = J_{2,i}(R_i)^2$$

where A_i is the i-th body's oblateness parameter.

Within the CR3BP, the leading oblateness term has two primary dynamical consequences: it shifts equilibrium locations and it perturbs the local stability. In the model with one oblate primary, analyses report systematic displacements of the five classical equilibria and corresponding changes in the stability conditions near both the collinear points and the triangular points (12, 28, 29).

Studies extended this in two directions. One combined oblateness with additional effects (30), and broadened primary shape modeling beyond axisymmetry (31). Another direction refined stability analysis in the oblate setting and explored stability under multiple small perturbations in the rotating-frame equations (19, 32, 33). Much of this literature assumed the oblateness parameters were small and developed results as perturbations of the classical CR3BP.

A key qualitative shift occurs when both primaries are treated as oblate. In this two-oblateness model, the classical single Routh mass-ratio threshold for triangular-point stability is replaced by a numerically evaluated stability boundary in the full parameter space $\mu_{cr}(A_1, A_2)$ so stability is naturally presented as surfaces rather than a single critical value (34).

Because the equilibrium and stability conditions become algebraically more complex once both oblateness terms are retained, results are commonly mapped numerically over admissible (μ, A_1, A_2), with primary attention on L4 and L5, while the collinear points remain linearly unstable.

Drag forces

Drag forces provide a natural and physically important departure from the classical CR3BP, because they introduce dissipation and therefore break the conserved quantities (most notably the Jacobi integral) that organize motion in the conservative model. In the rotating frame, one may still speak of "equilibrium" configurations, but these are no longer stationary points of an effective potential in the usual sense. Instead, they become drag-displaced equilibria whose locations depend on the drag law and whose linear stability depends on the local derivatives of that drag field at the displaced point.

One historical strand treats drag forces for small particles - radiative drag. The Poynting-Robertson (PR) effect arises when an orbiting grain absorbs and re-emits radiation, producing a small tangential component of force that removes angular momentum and causes inward orbital decay (35). In the CR3BP setting, this effect was incorporated into early equilibrium stability studies of dust motion under radiation pressure, where it was shown that Lagrange points became unstable under such forces (36).

As an example of another dissipative force analysis, Jeffreys (37) recognized that even weak dissipation can fundamentally change the status of the triangular equilibria. He treated an external drag proportional to the particle's velocity in the rotating frame and concluded that the triangular points L4 and L5 become unstable under such dissipation. Yoder (17) considered possible mechanisms for Trojan formation, most of which involved dissipation. Later, the general problem of the effects of dissipative processes on stability was discussed (38); in their orbital evolution discussion on the Janus and Epimetheus system they stated that a detailed analysis of dissipative behavior is required, not from simple energy arguments like what previous papers claimed (37).

Some studies focused on numerical analysis. Peale (39), for example, examined Trojan precursors near proto-Jupiter under a solar-nebula drag model and by numerical integration of specific cases showed that L4 and L5 could be stable to this drag force. In a different more analytical direction, and with a more general approach, Murray (18) showed the futility of energy arguments, using a dynamical-systems approach that treated drag forces in the CR3BP at the level of the equations of motion, deriving how different drag laws displace the equilibrium points, how equilibria can move along curves and potentially merge or disappear as drag increases, and how linear stability criteria depend on the functional form of the drag.

Murray (18) treats drag as a general non-conservative perturbation to the planar CR3BP and uses it to build a unified picture of how the five equilibrium points are displaced and how their linear stability changes. Working in the rotating frame, he rewrites the equations of motion with an arbitrary drag force (rather than specializing immediately to a single physical model) and tracks how the Jacobi constant is no longer conserved once drag is present. Equilibria in the dragged problem are found by a first-order approximation for small shifts, assuming the drag force is not as dominant as the gravitational forces. He then derives explicit first-order formulas for the shifts of L1 through L5 in terms of those force components, and shows the displaced equilibria move along certain geometric paths as drag strength increases, with characteristic events such as equilibria approaching one another, merging, and disappearing. Furthermore, he linearizes the drag dynamics about a displaced equilibrium and obtains a quartic characteristic polynomial whose coefficients can be expressed through partial derivatives of the drag force function; this yields stability conditions for L4 and L5 that are most naturally evaluated from the drag Jacobian at the displaced point. Notably, he shows that no drag force can stabilize the collinear points: in the collinear case the structure of the linearized problem guarantees at least one eigenvalue with positive real part, so L1, L2 and L3 remain linearly unstable even after the equilibrium is displaced.

Within this general framework, Murray discusses several examples, using them to highlight the need to consider the forces dynamically, and not to rely on energy-based arguments. Additionally, he focuses on the physically relevant Poynting–Robertson drag, applying the same methods to the triangular points; his systematic approach confirms the results of previous works (37) that L4 and L5 are destabilized.

Another interesting and physically relevant drag force considered is Peale's nebular gas drag (39). In applying his general displaced-equilibrium formalism to nebular gas drag, Murray specializes to the drag used by Peale, in which the dissipative force is proportional to the planetesimal's velocity relative to the gas and the gas itself is described by a sub-Keplerian rotation law together with a radius-dependent density structure (details of the specific complex functional forms are excluded here, since the equilibrium and stability consequences are the focus). By transforming Peale's inertial-frame drag into rotating-frame components and evaluating these at equilibrium, Murray shows that the equilibrium conditions can be cast into the same structural form as his broader inertial drag class, so that the approximate methods developed earlier in the paper remain applicable. This identification allows him to interpret Peale's numerical findings in the language of displaced Lagrange points: the triangular points follow the same characteristic displacement paths, and sufficiently strong nebular drag can shift a triangular equilibrium through large angular offsets and, in extreme regimes, lead to a disappearance.

At the same time, the nebular setting makes clear why a complete stability treatment becomes far more difficult than an abstract drag case. In Peale's formulation the drag force depends on many physical parameters (particle size, drag coefficient, gas density profile, gas rotation profile, and scaling constants), and the dependence on radius is through nonlinear functions that enter both the magnitude of the relative velocity and the drag direction. Murray therefore leaves a full stability analysis for Peale's model beyond the scope of his paper, while explicitly emphasizing that his linear-stability methods should, in principle, still apply. In practice, this pushes the stability problem toward numerical evaluation of the linearized coefficients over parameter space, rather than closed-form inequalities.

EFFECTS ON PERIODIC ORBITS

Radiation pressure and Oblateness

Having established how radiation pressure and oblateness shift equilibria and stability regions, the next question is how the classical periodic-orbit families (e.g., the Lyapunov family around L1 in Figure 2) deform under these conservative perturbations.

In the photogravitational CR3BP, a representative orbit-family treatment is (40), which explicitly formulates the problem with radiating primaries and focuses on constructing families of periodic orbits under radiation pressure. Pathak *et al.* (41) analyzed the first order exterior resonant orbits and the first, third and fifth order interior resonant periodic orbits in a radiation pressure-modified system. Numerical continuation studies further show that radiation parameters systematically deform planar periodic families; for example, Papadakis (42) determines all families of planar symmetric simple-periodic orbits (in an equal-mass, equal-radiation case) numerically, illustrating how radiation enters as a control parameter that reshapes families. Across these studies, the dominant outcome is deformation and parameter-dependent reparameterization of existing families, rather than disappearance of the families themselves.

Since radiation acts mainly as an effective rescaling in the conservative problem, it is useful to contrast this 'family deformation' behavior with oblateness, which modifies the potential's higher-order structure. Abouelmagd, García Guirao and Llibre (43) characterize when Poincaré's classical first- and second-kind periodic orbits of the planar CR3BP can be extended to perturbed planar CR3BP models, with special emphasis on perturbations due to zonal harmonics (i.e., oblateness and higher harmonics). More orbit-family–direct work includes Mittal, Ahmad and Bhatnagar (44), who compute periodic orbits generated by Lagrangian solutions when one primary is oblate, determining periodic orbits across parameter sets (mass ratio, Jacobi constant, oblateness factor). Related computations of critical or transition structures in the oblate problem include (45), which develops a series of horizontally critical symmetric periodic orbits in the restricted problem when the more massive primary is an oblate spheroid and evaluates their stability. Taken together, these results emphasize that zonal-harmonic terms primarily shift stability and criticality along established families, so the practical deliverables are stability maps and numerically continued branches rather than closed-form family descriptions.

Because orbit families in perturbed CR3BP models are typically obtained via continuation or shooting, most of the modern exploration of conservative effects is intrinsically numerical, and it is common to investigate multiple perturbations simultaneously. Patel *et al*. (21) treat resonant periodic orbits in a CR3BP where both primaries are radiating and oblate, and they organize their results as a parameter–response study of the geometry of resonant periodic orbits. After formulating the perturbed equations, they numerically analyze interior and exterior first-order resonant periodic orbits by tracking the initial position of the orbit and the size of loops as functions of the perturbation parameters, both individually and in combinations, and then as functions of dynamical descriptors such as the Jacobi constant, mass factor, resonance order, and number of loops. They then summarize the importance of each parameter: radiation pressure shifts the initial condition x toward the smaller primary and reduces loop size, whereas oblateness shifts x toward the bigger primary and increases loop size. They use these parameter sweeps to provide a compact sensitivity picture: how resonant-family geometry responds when radiation and oblateness are varied jointly, and how the same trends reorganize across interior vs. exterior resonances and across different Jacobi constants and mass factors.

While the emphasis in (21) is on parameter sweeps, other works extend the same framework with additional controls and bifurcation structure. For example, Gao and Wang (20) study a perturbed R3BP motivated by a luminous eclipsing binary, where the model includes radiation pressure, oblateness, and time-varying mass (modelled using the Gyldén-Meshcherskii problem – (46, 47, 48). First, they compute and visualize the system via zero-velocity surfaces and then explore dynamical responses via bifurcation diagrams across a set of perturbation parameters. Their bifurcation-based approach is used to diagnose parameter sensitivity in the combined model (including strong dependence on the varying-mass parameter κ), while radiation and oblateness contributions enter as additional control parameters shaping the resulting branches. They also derive second- and third-order approximate analytical periodic solutions near the collinear libration points using the Lindstedt–Poincaré method, finding improved agreement between the two approximation orders for smaller values of the changing-mass parameter and better cross-order agreement in the three-dimensional case than in the planar case.

Drag forces

In a dissipative system, true closed periodic orbits typically do not persist because energy is continually lost. Unlike the classical restricted three-body problem where families of periodic orbits abound, adding a drag force causes those orbits to shrink or spiral inward instead of repeating indefinitely. In fact, an analytical study by Margheri *et al*. proved that the standard periodic solutions of the planar CR3BP cannot be continued when a generic drag term is introduced (49). This work also established general conditions under which no small periodic oscillations (limit cycles) emerge around the equilibrium points, except in special cases of very specific drag forms. These findings agree with earlier numerical investigations by Celletti *et al*., who reported that they found no closed orbits in the R3BP when a drag force was included (50).

Accordingly, results on "periodic orbits" under drag are typically reported as decaying or quasi-periodic trajectories that resemble classical families only over finite times, or genuinely dissipative periodic attractors that arise only for special drag laws.

Although a general closed-form theory is absent, researchers have examined specific types of drag forces to understand how known periodic orbits are altered or

eliminated. One well-studied example is the Poynting–Robertson drag. When PR drag is included in the CR3BP, the classic halo and Lissajous orbits around Lagrange points no longer remain periodic: they shrink in size and take longer to complete each loop as drag increases. For instance, Pal and Kushvah added PR drag and solar wind drag to a halo orbit near the Sun–Earth L1 point and found that the trajectory's amplitude contracts and its period increases compared to the no-drag case (51). In their third-order analytical expansion (using a Lindstedt–Poincaré method), the authors could approximate the modified orbit with drag. However, this solution is a quasi-periodic decaying spiral. Consistent with this, Margheri *et al.* note that under PR drag the triangular libration points L4 and L5 (which in the conservative case allow stable tadpole orbits) turn into unstable points for all mass ratios.

While some drag laws primarily destroy conservative orbit families, others can generate dissipative periodic behavior. In particular, Stokes drag (proportional to velocity, often used for motion in a thin atmosphere or gas) does not generally preserve the families of periodic orbits; instead, it can generate dissipative periodic attractors. Margheri *et al*. treat Stokes drag as a distinct dissipative perturbation and show that, unlike the PR case, the triangular equilibria can enter a regime where a Hopf bifurcation occurs, producing small-amplitude periodic solutions around the equilateral points for appropriate drag parameters. Their conclusions are consistent with the numerical results reported by Celletti *et al*. (50).

Beyond these cases, various authors have studied drag-induced orbital decay and resonance trapping rather than strict periodic orbits. For instance, Beaugé and Ferraz-Mello investigated how PR drag can draw particles into mean-motion resonances temporarily, but ultimately the drag causes escape from resonance (52). Liou *et al*. likewise modeled dust grains under solar radiation and wind drag in the CR3BP and confirmed that grains spiral toward the Sun over time (53).

CONCLUSION

The topic of physical modifications to the CR3BP is relevant. Libration-point mission design is sensitive to perturbations absent from the ideal CR3BP, particularly solar radiation pressure and non-spherical gravity. For JWST in the Sun–Earth–Moon L2 region, operational flight-dynamics models include an Earth geopotential expansion (EGM96 30 × 30) and a high-fidelity, attitude-dependent radiation pressure model, because both materially affect orbit determination and station-keeping targeting (54). Analyses on the JWST dynamics require high accuracy and, in turn, have validated the theoretical model (54). In planetary-formation contexts, drag-perturbed CR3BP models provide a mechanism-level link between disk conditions and the survival of co-orbital reservoirs. In a solar-nebula environment, gas drag displaces the effective L4 and L5 equilibria and drives size-dependent evolution of libration amplitudes; outcomes depend on disk structure and its time evolution, with implications for which precursor sizes remain trapped through dispersal and whether leading and trailing asymmetries emerge (39). The long-term existence and phase-space structure of Trojan asteroid populations are well explained within the CR3BP framework and its extensions, with observed libration and stability properties consistent with theoretical predictions for co-orbital motion (55).

The comparative summary in Table 1 clarifies why results across perturbation models do not combine into a single uniform framework. In conservative settings, the dominant outputs are equilibrium locations and linear-stability regions mapped over parameter space. In dissipative settings, a Jacobi-like invariant is unavailable and classical orbit families need not persist, so results are more often local approximations around displaced equilibria and time-domain behavior.

In the photogravitational CR3BP, radiation is treated as a conservative rescaling of inverse-square attraction and dissipative radiative effects are neglected. This

Table 1. *Comparative summary of typical qualitative outcomes, methods, and computational challenges across three representative perturbation classes in the CR3BP.*

Item	Radiation pressure	Oblateness	Drag force
Type	Conservative	Conservative	Dissipative; Jacobi constant breaks
Lagrange point location	Collinear: x shift; Triangular: (x, y) shift	Collinear: x shift; Triangular: (x, y) shift	All points displaced; typically (x, y) shift

Continued Table 1. *Comparative summary of typical qualitative outcomes, methods, and computational challenges across three representative perturbation classes in the CR3BP.*

Item	Radiation pressure	Oblateness	Drag force
Lagrange point stability	parameter-dependent regions	modified Routh criterion $\mu < \mu_{cr}(A_1, A_2)$	modified criteria; force-law dependent
Extra equilibria	4 possible extraplanar points	–	–
Periodic orbits	families persist; deform	families persist; deform	decay
Methods	equilibrium equations; parameter maps; numerical solves	root-finding; stability-region maps; zero-velocity surfaces; Lindstedt–Poincaré	small-dissipation expansion; Newton iteration; integration; Hopf criteria
Computational challenges	multi-parameter sweep	algebraic complexity; multi-parameter sweep	stiffness; derivative-heavy; force-law sensitivity; high-dimensional sweeps

makes equilibrium existence and linear stability well posed as a multi-parameter classification problem, but it limits relevance for decay; some parameter regimes also require case-by-case physical justification (e.g., radiation-dominated attraction).

For two-oblateness models, stability boundaries for the triangular equilibria are typically obtained numerically over (J1, J2, μ), so μ_{cr} is a computed surface instead of a closed-form threshold (35). In Lyapunov special cases, first-order theory can be inconclusive and higher-order terms change the stability outcome (19). For combined-perturbation models, zero-velocity surfaces and bifurcation diagrams provide global constraints, while Lindstedt–Poincaré expansions give local periodic-orbit approximations near collinear points that remain parameter sensitive (20).

Drag models impose the strongest restrictions. Displaced-equilibrium theory assumes small dissipation and yields force-law-dependent stability criteria (18). More fundamentally, periodic solutions of the planar CR3BP generally cannot be continued into dissipative variants under broad conditions, and in Poynting–Robertson drag the displaced triangular equilibrium can be hyperbolically unstable in the small-dissipation regime (49). Higher-order series under drag often produce quasi-periodic, decaying spirals rather than closed periodic orbits (51). In nebular-drag applications, full stability treatments are frequently deferred because dimensionality and parameter coupling dominate (18, 39). Additionally, even when one defines a critical disk surface density (or analogous single control parameter) for loss of triangular-point stability under fixed remaining nebular parameters, the boundary typically remains computationally intensive because the constants entering the stability criterion encode the full nonlinearity of the model.

These limitations point to concrete gaps. First, conservative radiation-pressure classifications are still rarely linked to radiative-drag evolution, even though many applications require both. Second, in two-oblateness and combined-perturbation models, stability beyond linear theory is not mapped systematically across admissible parameter ranges. Third, in drag-perturbed variants, studies often stop at local displaced-equilibrium or bifurcation results and do not connect them to global outcomes under physically constrained, high-dimensional nebular drag laws.

Combined models increase dimensionality and often introduce stiffness, so brute-force multi-parameter sweeps scale poorly. Effective workflows therefore pair analytic reduction with continuation or boundary tracking in conservative cases, and sensitivity-aware integration in dissipative cases. Typical toolchains include continuation and bifurcation packages (AUTO, MATCONT, COCO, BifurcationKit) and integration and sensitivity stacks (MATLAB, SciPy, DifferentialEquations.jl with automatic differentiation), chosen according to whether families and stability regions (conservative) or decay, capture or attractors (dissipative) are sought.

ACKNOWLEDGEMENTS

Thank you for the guidance of Professor Ryan Farber from Purdue University Fort Wayne in the development of this research paper.

CONFLICT OF INTEREST

The author declares that there are no conflicts of interest related to this work.

REFERENCES

1. Gutzwiller MC. Moon-Earth-Sun: the oldest three-body problem. *Rev Mod Phys*. 1998; 70 (2): 589-639. https://doi.org/10.1103/RevModPhys.70.589
2. Bruns EH. Über die Integrale des Vielkörper-Problems. *Acta Math*. 1887; 11: 25-96. https://doi.org/10.1007/BF02612319
3. Poincaré H. Les méthodes nouvelles de la mécanique céleste. Vol 1. Paris: Gauthier-Villars et fils; 1892. https://doi.org/10.1090/S0002-9904-1892-00082-1
4. Brouwer D, Clemence GM. Methods of celestial mechanics. New York: Academic Press; 1961.
5. Szebehely V. Theory of orbits: the restricted problem of three bodies. New York: Academic Press; 1967. https://doi.org/10.1016/B978-0-12-395732-0.50016-7
6. Marchal C. The three-body problem. Amsterdam: Elsevier; 1990.
7. Lagrange JL. Essai sur le problème des trois corps. Prix de l'Académie Royale des Sciences de Paris; 1772.
8. Gascheau G. Examen d'une classe d'équations différentielles et application à un cas particulier du problème des trois corps. *C R Acad Sci Paris*. 1843; 16: 393-394.
9. Jacobi CGJ. Sur le mouvement d'un point et sur un cas particulier du problème des trois corps. *C R Acad Sci Paris.* 1836; 3: 59-61.
10. Farquhar RW. Lunar Communications with Libration-Point Satellites. *Spacecraft and Rockets*. 1967; 4: 1383-1384. https://doi.org/10.2514/3.29095
11. Rabe E. The Trojans as escaped satellites of Jupiter. *Astron J.* 1954; 59: 433-438. https://doi.org/10.1086/107058
12. Sharma RK, Subba Rao PV. Stationary solutions and their characteristic exponents in the restricted three-body problem when the more massive primary is an oblate spheroid. *Celest Mech*. 1976; 13: 137-149. https://doi.org/10.1007/BF01232721
13. Simmons JFL, McDonald AJ, Brown JC. The restricted three-body problem with radiation pressure. *Celest Mech*. 1985; 35: 145-187. https://doi.org/10.1007/BF01227667
14. Schuerman DW. The restricted three-body problem including radiation pressure. *Astrophys J.* 1980; 238: 337-342. https://doi.org/10.1086/157989
15. Chernikov YuA. The photogravitational restricted three-body problem. *Sov Astron*. 1970; 14 (1): 176-181.
16. Horedt GP. A variable mass of the primaries and librations around the triangular points. *Celest Mech*. 1974; 10: 319-326. https://doi.org/10.1007/BF01586861
17. Yoder CF. Notes on the origin of the Trojan asteroids. *Icarus*. 1979; 40 (3): 341-344. https://doi.org/10.1016/0019-1035(79)90024-1
18. Murray CD. Dynamical effects of drag in the circular restricted three-body problem: 1. Location and stability of the Lagrangian equilibrium points. *Icarus*. 1994; 112 (2): 465-484. https://doi.org/10.1006/icar.1994.1198
19. Subba Rao PV, Sharma RK. Effect of oblateness on the non-linear stability of L4 in the restricted three-body problem. *Celest Mech Dyn Astron*. 1996; 65: 291-312. https://doi.org/10.1007/BF00053510
20. Gao F, Wang Y. Approximate Analytical Periodic Solutions to the Restricted Three-Body Problem with Perturbation, Oblateness, Radiation and Varying Mass. *Universe*. 2020; 6 (8): 110. https://doi.org/10.3390/universe6080110
21. Patel BM, Pathak N, Abouelmagd E. Analysis of resonant periodic orbits in the framework of the perturbed restricted three bodies problem. *Universe*. 2023; 9 (5): 239 https://doi.org/10.3390/universe9050239
22. Radzievskii VV. The restricted problem of three bodies taking into account light pressure. *Astron Zh*. 1950; 27: 250.
23. Radzievskii VV. The space photogravitational restricted three-body problem. *Astron Zh*. 1953; 30 (3): 265-273.
24. Perezhogin AA. Stability of the sixth and seventh libration points. *Sov Astron Lett.* 1976; 2 (5): 174-175.
25. Legendre A-M. Recherches sur l'attraction des sphéroïdes homogènes. *Mém Acad R Sci Paris*. 1785; 10: 411-435.
26. Brouwer D. Solution of the problem of artificial satellite theory without drag. *Astron J.* 1959; 64: 378-397. https://doi.org/10.1086/107958
27. Kozai Y. The motion of a close Earth satellite. *Astron J.* 1959; 64: 367-377. https://doi.org/10.1086/107957
28. Vidyakin VV: Soviet Astron. *Astron. J.* 1974; 18: 641. Translated from Astron Zh. 51, 1087-1094
29. Sharma RK, Subba Rao PV. Effect of oblateness on triangular solutions at critical mass. *Astrophys Space Sci.* 1979; 60: 247-250. https://doi.org/10.1007/BF00644329
30. Singh J, Ishwar B. Stability of triangular points in the generalized photogravitational restricted three-body problem. *Bull Astron Soc India*. 1999; 27: 415-424.
31. Sharma RK, *et al*. Existence and stability of libration points in the restricted three-body problem when the primaries are triaxial rigid bodies. *Celest Mech Dyn Astron*. 2001; 79: 119-133. https://doi.org/10.1023/A:1011168605411
32. AbdulRaheem A, Singh J. Combined effects of perturbations, radiation and oblateness on the periodic orbits in the restricted three-body problem. *Astrophys Space Sci.* 2008; 317 (1): 9-13. https://doi.org/10.1007/s10509-008-9841-4

33. Singh J. Combined effects of perturbations, radiation, and oblateness on the nonlinear stability of triangular points in the restricted three-body problem. *Astrophys Space Sci*. 2011; 332: 331-339. https://doi.org/10.1007/s10509-010-0546-0
34. Arredondo JA, Guo J, Stoica C, Tamayo C. On the restricted three body problem with oblate primaries. *Astrophys Space Sci.* 2012; 341 (2): 315-322. https://doi.org/10.1007/s10509-012-1085-7
35. Robertson HP, Russel HN. The dynamical effects of radiation in the solar system. *Mon Not R Astron Soc*. 1937; 97: 423-437. https://doi.org/10.1093/mnras/97.6.423
36. Colombo G, Lautman DA, Shapiro II. The Earth's dust belt: Fact or fiction? 2. Gravitational focussing and Jacobi capture. *J. Geophys. Res.* 1966; 71: 5705-5717. https://doi.org/10.1029/JZ071i023p05705
37. Jeffreys H. 1929. The Earth, 2nd ed. Cambridge Univ. Press, Cambridge
38. Yoder CF, Colombo G, Synnott SP, Yoder KA. Theory of motion of Saturn's coorbiting satellites. *Icarus.* 1983; 53: 431-443. https://doi.org/10.1016/0019-1035(83)90207-5
39. Peale SJ. The effect of the nebula on the Trojan precursors of Jupiter. *Icarus.* 1993; 106 (2): 308-322. https://doi.org/10.1006/icar.1993.1173
40. Elipe A, Lara M. Periodic orbits in the restricted three body problem with radiation pressure. *Celest Mech Dyn Astron*. 1997; 68: 1-11. https://doi.org/10.1023/A:1008233828923
41. Pathak N, Thomas VO, Abouelmagd EI. The perturbed photogravitational restricted three-body problem: Analysis of resonant periodic orbits. *Discrete Contin Dyn Syst Ser S*. 2019; 12 (4&5): 849-875. https://doi.org/10.3934/dcdss.2019057
42. Papadakis KE. Families of periodic orbits in the photogravitational three-body problem. *Astrophys Space Sci.* 1996; 245: 1-13. https://doi.org/10.1007/BF00637799
43. Abouelmagd EI, García Guirao JL, Llibre J. Periodic orbits for the perturbed planar circular restricted 3-body problem. *Discrete Contin Dyn Syst Ser B.* 2019; 24 (3): 1007-1020. https://doi.org/10.3934/dcdsb.2019003
44. Mittal A, Ahmad I, Bhatnagar KB. Periodic orbits generated by Lagrangian solutions of the restricted three body problem when one of the primaries is an oblate body. *Astrophys Space Sci*. 2009; 319: 63-73. https://doi.org/10.1007/s10509-008-9942-0
45. Perdios EA, Kalantonis VS. Critical periodic orbits in the restricted three-body problem with oblateness. *Astrophys Space Sci.* 2006; 305: 331-336. https://doi.org/10.1007/s10509-005-9035-2
46. Gyldén, H. Die bahnbewegungen in einem systeme von zwei Körpern in dem falle, dass die massen veränderungen unterworfen sind. *Astron. Nachr.* 1884; 109: 1-6. https://doi.org/10.1002/asna.18841090102
47. Bekov AA. Periodic solutions of the Gylden-Meshcherskii problem. *Astron. Rep.* 1993; 37: 651-654.
48. Bekov AA, Momynov SB. Parametric solutions of the Gyldén-Meshcherskii problem. *Int J Non-Linear Mech.* 2019; 116: 195-199. https://doi.org/10.1016/j.ijnonlinmec.2019.06.009
49. Margheri A, Ortega R, Rebelo C. Some analytical results about periodic orbits in the restricted three body problem with dissipation. *Celest Mech Dyn Astron.* 2012; 113: 279-290. https://doi.org/10.1007/s10569-012-9415-1
50. Celletti A, Stefanelli L, Lega E, Froeschlé C. Some results on the global dynamics of the regularized restricted three-body problem with dissipation. *Celest Mech Dyn Astron.* 2011; 109 (3): 265-284. https://doi.org/10.1007/s10569-010-9326-y
51. Pal AK, Kushvah BS. Geometry of halo and Lissajous orbits in the circular restricted three-body problem with drag forces. *Mon Not R Astron Soc*. 2015; 446 (1): 959-972. https://doi.org/10.1093/mnras/stu2100
52. Beaugé C, Ferraz-Mello S. Capture in exterior mean-motion resonance due to Poynting-Robertson drag. *Icarus*. 1994; 110: 239-260. https://doi.org/10.1006/icar.1994.1119
53. Liou J-C, Zook HA, Jackson AA. Radiation pressure, Poynting-Robertson drag, and solar wind drag in the restricted three-body problem. *Icarus*. 1995; 116: 186-201. https://doi.org/10.1006/icar.1995.1120
54. Logan J, Verma AK, Cavanaugh S, Yu A. James Webb Space Telescope navigation optimization challenges. International Symposium on Space Flight Dynamics. 2024. https://ntrs.nasa.gov/citations/20230018630
55. Robutel P, Souchay J. An introduction to the dynamics of Trojan asteroids. In: Dynamics of Small Solar System Bodies and Exoplanets. *Lecture Notes in Physics.* 2010; 790: 195-227. https://doi.org/10.1007/978-3-642-04458-8_4